

Surfactant-Free Synthesis of Carbon-Supported Au@Pt Nanocatalysts for Methanol Oxidation

Guangju Zhou¹, Yuanming Xu¹, Yunzhi Fu^{1,*}, Yun Yang^{2,*}, Yucang Zhang¹

¹Hainan University College of Materials and Chemical Engineering HaiNan Haikou 570228

²Nanomaterials and Chemistry Key Laboratory, Wenzhou University, Wenzhou, Zhejiang 325027, P. R. China

*E-mail: jnfuz@163.com; bachier@163.com

Received: 19 February 2014 / Accepted: 27 March 2014 / Published: 14 April 2014

We developed a facile and low-cost method for preparing carbon-supported Au@Pt nanocatalyst with high catalytic activity. Our synthetic route does not involve using any surfactant. Carbon black acts as both catalyst supporter and stabilizing agent. First, carbon-supported Au nanoparticles (NPs) are prepared and then Pt deposition occurs selectively on Au NPs surfaces, forming Au@Pt nanocatalysts. The reaction temperature and reducing agent play important roles in the growth of Au@Pt nanocatalyst. Low reaction temperature causes slow reaction. Too high temperature or agents with strong reducing ability generate formation of Pt NPs due to the additional nucleation. The electrocatalytic performances of prepared catalysts show that they have higher activity and stability than commercial carbon-supported Pt in the methanol Oxidation reaction.

Keywords: core@shell, seeded growth, Au, Pt, methanol oxidation, nanocatalyst

1. INTRODUCTION

Noble core@shell NPs attract much attention due to their potential applications in catalysis, optics and magnetic separation. [1-4] Numerous noble core@shell NPs have been prepared with different technologies, such as Au@Ag, Au@Pd, Au@Pt, Pd@Au, Ag@Ag. Among them, the synthesis of Au@Pt NPs is pursued extensively because they are potential catalyst of fuel cell. Au@Pt NPs are advantageous due to the following features. The synergistic effect of Au core and Pt shell can improve the performance of catalyst.[5] Besides, Pt is more expensive than Au and this strategy can low the cost of catalyst. Generally, the preparation of Au@Pt NPs often involves using seeded growth. That is to say, Au NPs are prepared first and then they serve as seeds for Pt deposition. In most

preparations of Au@Pt NPs, researchers use surfactant for controlled growth.[5] In practical application, the absorbed surfactant can reduce the catalytic ability of Au@Pt NPs. For this reason, the prepared Au@Pt NPs need purification to remove surfactants. To protect the purified Au@Pt NPs against aggregation, carbon is always employed as supporter to separate Au@Pt NPs. Purification surely increases cost and also generates waste water, indicating that surfactant-assisted synthesis is not good for mass production. Recently, Xu's group synthesized carbon-supported Fe@Pt NPs with a surfactant-free galvanic reaction.[6] This group also prepared Au@Ag NPs supported by inorganic complex through a similar technology. [7] Their studies demonstrate that the selective deposition and growth on seed surface are still favored without surfactant. If carbon-supported Au@Pt NPs catalysts could be prepared with such method, cost can be reduced significantly. Besides, because no surfactant is used, the catalytic ability of Au@Pt is not influenced negatively. Therefore, this might be a low-cost way to prepare highly active catalyst and putting more efforts into developing such methods is desirable. Herein, we demonstrate the surfactant-free synthesis of carbon-supported Au@Pt NPs can be achieved through carrying out seeded growth on carbon supporter. The ratio of Pt and Au is controllable through adjusting the amount of Pt precursor. More importantly, the activity of Au@Pt catalyst is enhanced and they have better performance than commercial carbon-supported Pt NPs. These features are good for mass production.

2. EXPERIMENTAL SECTION

H₂AuCl₄, H₂PtCl₆, ascorbic acid (AA), NaBH₄ and carbon-supported Pt (40 wt %,) were purchased from TCI. They are used as received and need no further purification. Deionized water (18.2 MΩ·cm) was prepared with Milli-Q Academic water purification system (Millipore Corp., Billerica, MA, USA) and used in all experiments.

2.1 The synthesis of carbon-supported Au NPs

Carbon-supported Au seeds were prepared following a reported method. In a typical synthesis, 20 mg H₂AuCl₄ was added to 20 mL ethanol or water containing 38 mg carbon black. Ultrasonic was used to obtain a homogenous dispersion. 1 mL ice-cold NaBH₄ aqueous solution (NaBH₄/Au=20) was added to reduce Au³⁺ to Au atom. After another 30 min reaction, the carbon-supported Au NPs product was separated by centrifugation and washed with water for several times to remove byproduct. The purified solid carbon-supported Au NPs was redispersed in 20 mL of water.

2.2 The preparation of carbon-supported Au@Pt catalyst

In a standard synthesis, the prepared carbon-supported Au NPs was mixed with a calculated amount of H₂PtCl₆ and ascorbic acid (reducing agent). Then the solution was heated in a 80 °C oil bath for overnight. The carbon-supported Au@Pt nanocatalysts were separated by centrifugation and

washed with water for several times to remove byproduct. The purified solid carbon-supported Au NPs was redispersed in 100 μL of water for methanol Oxidation reaction.

2.3 The characterizations of NPs

The preparation of the catalyst NPs ultrasonically dispersed in water or ethanol. For transmission electron microscopy (TEM) and high resolution transmission electron microscopy (HRTEM), corresponding products were deposited on Cu grids and then observed on Tecnai G2 F30 S-Twin TEM with 300 kV accelerating voltage, and analyzed using an X-ray energy-dispersive spectrometer (EDS). The electrochemical measurement was carried out on electrochemical workstation (CHI660d, CH Instruments).

2.4 Electrochemical measurements

Electrochemical measurements were carried out in the electrolyte (0.5 M H_2SO_4 and 0.5 M methanol) by using conventional three-electrode cells with a Pt flake of 1 cm^2 area as the counter electrode, an Ag/AgCl–KCl (saturated) electrode as the reference electrode, and a glassy carbon loaded with active nanocatalysts as the working electrode. Before each experiment, the glassy carbon electrode was grinding very clean with the slurry of alumina NPs, and washed with water, then ultrasound with ethanol, so that the electrode surface free of impurities. A 10 μL aliquot suspension of the catalyst was drop-cast onto the glassy carbon electrode and dried naturally. The catalyst was fixed on the electrode by depositing a layer of dilution Nafion. For comparison, Commercial platinum-carbon (40 wt.% Pt, E-TEK) catalyst was prepared according to the same way. The electrochemical performance of the electrodes was investigated by using a PARSTAT 30 Advanced Electrochemical System. During the time of the electrochemical tests, the first pair of electrodes should be an empty sweep in sulfuric acid solution. The cyclic voltammograms (CV) of methanol oxidation were measured at the scan rate of 20 mV/s in the potential range of -0.2–1.0 V at room temperature. The chronoamperometry curves were obtained by polarizing the electrode at 0.48–0.53 V for 2000 s in the above-mentioned electrolyte. Before each test, the solution was purged with N_2 for 5 min to eliminate the dissolved oxygen.

3. RESULTS AND DISCUSSIONS

3.1. The synthesis of Carbon-supported Au@Pt

Experimentally, a variety of carbon-supported Au@Pt were synthesized through controlling the ratio of Pt and Au at 80 $^\circ\text{C}$. Figure 1 (a) show the TEM images of the synthesized Au seed NPs. Clearly, Au NPs were well-dispersed on the carbon supporter and no significant aggregation was observed, indicating that carbon supporter has excellent dispersion effect. The HRTEM image shows the Au NP has single-crystalline feature and 0.24 nm interplane distance is assigned to the {111} of

Au. After Pt deposited selectively on Au NPs surface, the products shape had distinctive change. Besides, their shapes changed with the ratio of Pt and Au. For example, when the molar ratio of Pt and Au was 1.5, multi-branched Au@Pt NPs formed (Figure 1B). Besides, no spherical Au NPs were observed, implying that the selective growth of Pt on Au NPs surface dominates and changes the product shape. This also demonstrates that surfactant-free seeded growth is feasible. If the ratio increased to 2.5, the length of branches became longer (Figure 1C). [27, 28] With the ratio increasing to 3.5, highly branched Au@Pt nanostructures formed (Figure 1D). The HRTEM images of Pt branches show that they have core@shell structure and good crystalline feature (Figure 1B2, B3, C2, C3, D2, D3). Compared with surfactant-assisted synthesis, the growth in our system has no significant preference because there is no the soft-template effect of surfactant. [5] When surfactant molecules are present, they selectively absorb on some facets and therefore the growth on those positions is limited. As a result, products often have well-defined shape. [5]

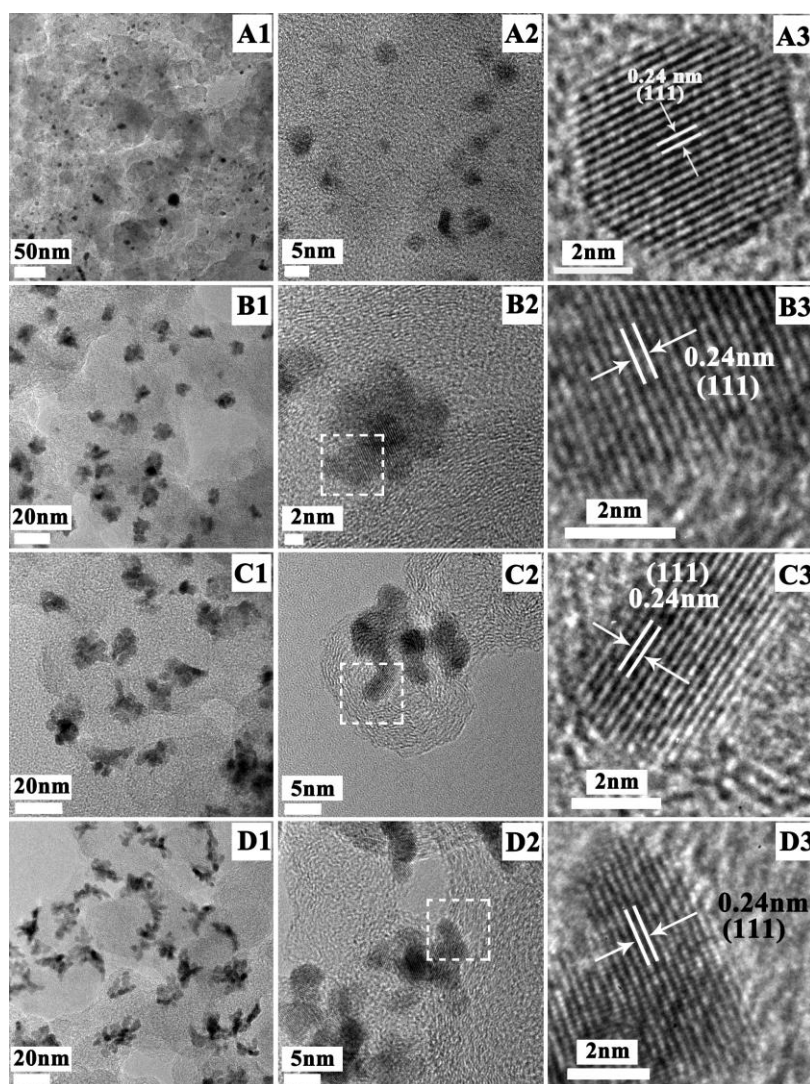


Figure 1. Typical TEM and HRTEM images of (A1-A3) carbon-supported Au@Pt nanostructures prepared using different ratios of Pt and Au; (B) 1; (C) 2; (D) 3. Image B3, C3 and D3 are the HRTEM images of selected area marked by the box in images B2, C2 and D2 respectively.

In order to confirm the structure of Au@Pt, EDS technology was used to analyze the composition of core and shell. When the signal was collected from the centre, both Pt and Au elements were observed (Figure 2A and B), indicating that the core contains Pt and Au. However, if the collected signal was from shell (branch), no Au element was observed (Figure 2C), indicating that branch is only composed of Pt element. The EDS pattern is consistent with above HRTEM results and provides hard evidence that the carbon-supported nanostructures are Au@Pt. STEM-EDS elemental mapping technology was also used to investigate the structure of Au@Pt. The Au and Pt elemental distribution images also clearly show that our products are core@shell (Figure 3).

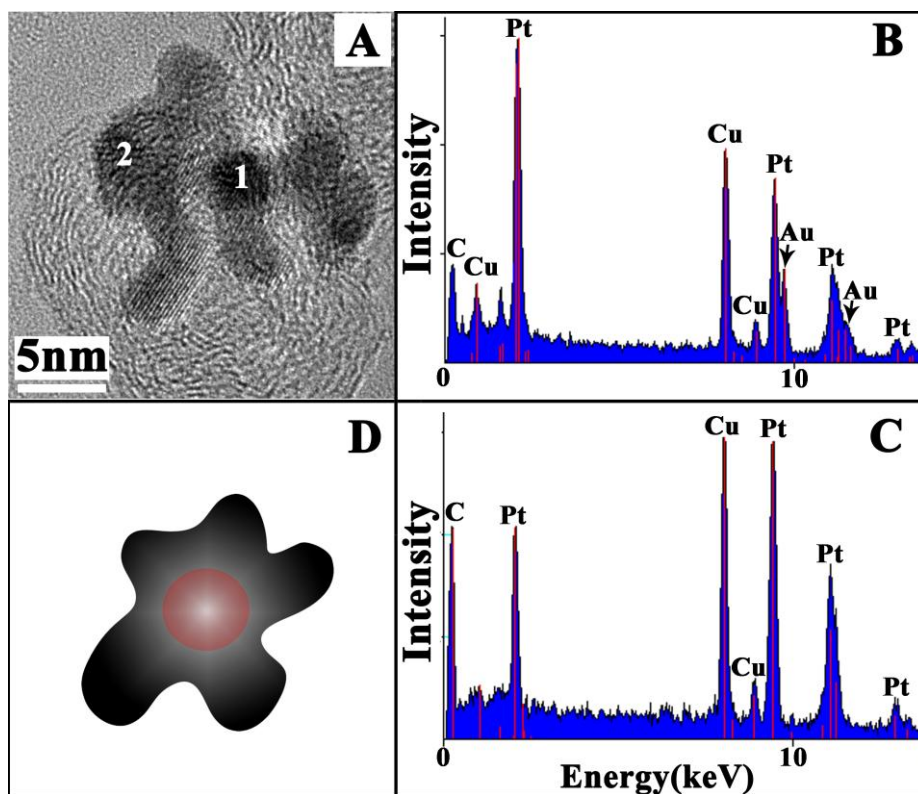


Figure 2. (A) Typical TEM images of one carbon-supported Au@Pt; (B-C) EDS patterns of selected area in Figure 1 (A); (D) Schematic image of Au@Pt nanostructure.

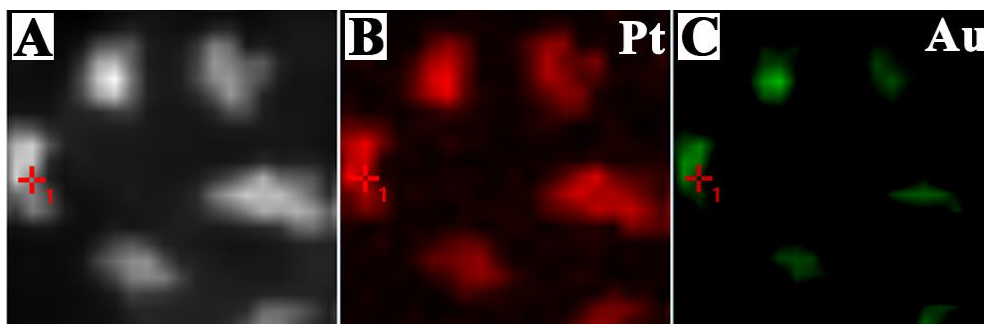


Figure 3. (A) HAADF image of carbon-supported Au@Pt; (B-C) corresponding elemental mapping of Pt and Au.

3.2 The effect of reaction temperature and reducing agent

The reaction temperature and reducing agent are important factors which affect the reaction kinetics and often used to tune the product shape. In the present study, we performed the syntheses of carbon-supported Au@Pt nanostructures at different reaction temperature.

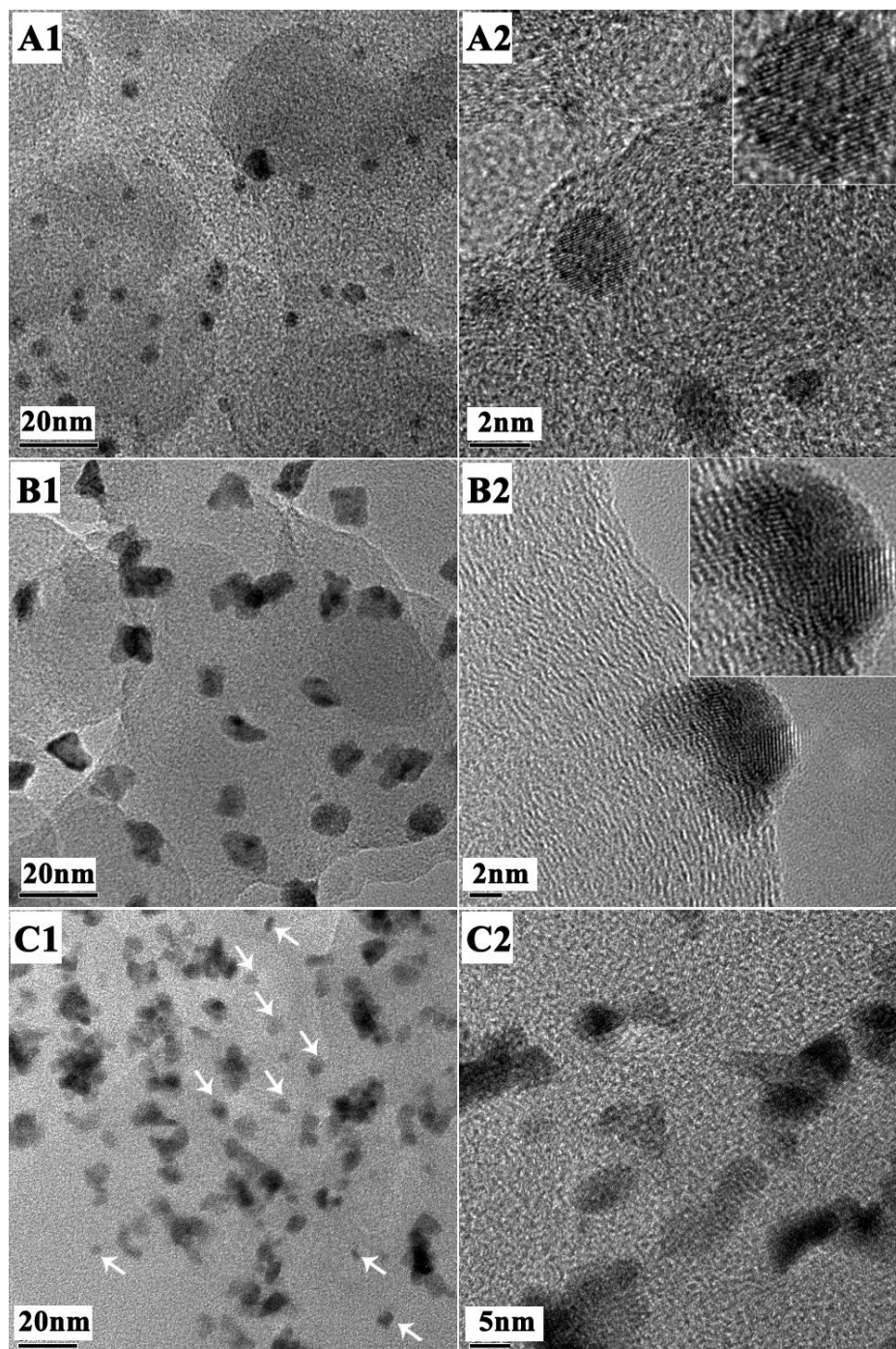


Figure 4. The TEM and HRTEM images of carbon-supported Au@Pt nanostructures prepared at different temperatures: (A1-A2) 20 °C; (B1-B2) 50 °C; (C1-C2) 120 °C. Insets in Figure 4A2 and B2 are the HRTEM images. The ratio of Pt and Au is 3.

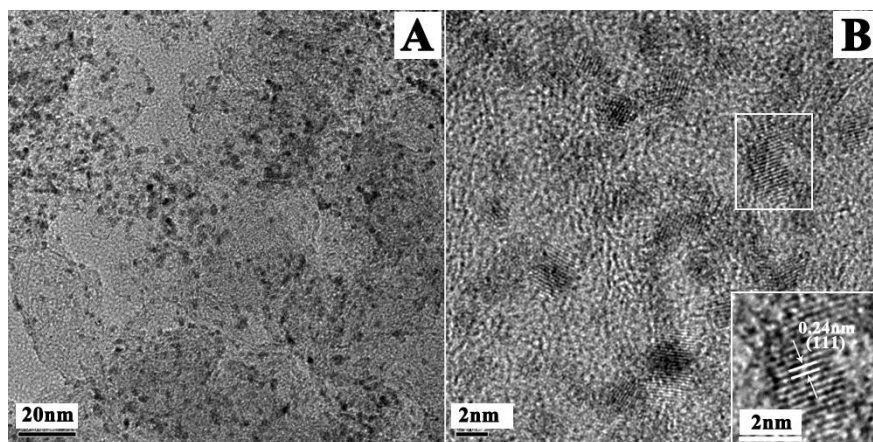


Figure 5. The TEM and HRTEM images of carbon-supported Au@Pt nanostructures prepared using NaBH_4 as reducing agent at $20\text{ }^\circ\text{C}$. Insets in Figure 5B are the HRTEM images of area marked by the box.

When the preparation was carried out at $20\text{ }^\circ\text{C}$, the product had no significant change and still spherical shape, indicating that no reduction from Pt^{4+} to Pt^0 occurred. Because ascorbic acid is weak reducing agent, it is difficult to reduce Pt^{4+} to Pt^0 at low temperature. When reaction temperature was increased to $50\text{ }^\circ\text{C}$, branched Au@Pt products formed (Figure 4B). However, compared with the products prepared at $80\text{ }^\circ\text{C}$ (Figure 1D), they are less branched, indicating that the reaction is still slow at $50\text{ }^\circ\text{C}$. If the synthesis was carried out in a $120\text{ }^\circ\text{C}$ autoclave, the products were polydispersed and lots of small sized NPs formed (Figure 4C), indicating that additional nucleation happens in this case. Above results show that the appropriate reaction temperature is $80\text{ }^\circ\text{C}$. Temperature lower than $80\text{ }^\circ\text{C}$ causes slow growth and too high temperature favors the additional nucleation. It is understandable that high temperature accelerates the reduction of Pt^{4+} to Pt^0 and produces high level of Pt^0 . For this reason, there is no enough nucleation sites for all Pt atoms on seeds surface. Additional nucleation happens consequently. As well as reaction temperature, reducing agent also has important roles on the products. If NaBH_4 with strong reducing ability acted as reducing agent, the fast reduction of Pt^{4+} to Pt^0 occurred even at room temperature (Figure 5), which caused very significant additional nucleation. As a result, the density of particles increased greatly. Above result demonstrates that the ascorbic acid with weak reducing ability is critical to the growth of carbon-supported Au@Pt nanostructures.

3.3 The catalytic properties in Oxidation of methanol

The electrochemical performances of the carbon-supported Au@Pt catalysts were tested in methanol oxidation as shown in Figure 6 (All catalysts with 40 wt.% Pt loading amount). Figure 6 A shows the typical cyclic voltammograms (CVs) of methanol oxidation by using prepared carbon-supported Au@Pt and commercial carbon-supported Pt as catalysts in a solution containing 0.5 M H_2SO_4 and 0.5 M methanol at room temperature. In all cases, two obvious anodic peaks related with the methanol Oxidation reaction features during the positive and negative sweeps, were clearly observed. All Au@Pt catalysts have higher catalytic peak current than commercial carbon-supported

Pt (283 mA/mg), indicating that the catalysts prepared using our method have better activity in the methanol Oxidation reaction. The high activity of branched Au@Pt catalysts possibly is due to present atomic defect and high index facet on their surface [31-32]. Besides, the catalytic abilities of catalysts significantly depend on the ratio of Pt and Au. For example, the catalytic peak current density of the carbon-supported Au@Pt (Pt:Au=1:1) in the positive direction sweep is the highest (464 mA/mg). In case of carbon-supported Au@Pt catalyst (Pt:Au=3:1), 355 mA/mg peak current was observed. However, when the Au@Pt catalyst (Pt:Au=1:3), a 397 mA/mg catalytic peak current was obtained. Above results clearly show that there are synergetic effects between Au and Pt in the methanol Oxidation reaction [33]. However, when the thickness of Pt shell is too large, the synergetic effect is lost. The time-current curve shown in Fig 6 B suggests that the catalyst (Pt:Au=1:1) also have the best stability and that (Pt:Au=1:3) takes second place. The catalyst (Pt:Au=3:1) has the worst stability. However, in all cases, the present Au core plays important roles on the stability in the methanol Oxidation reaction.

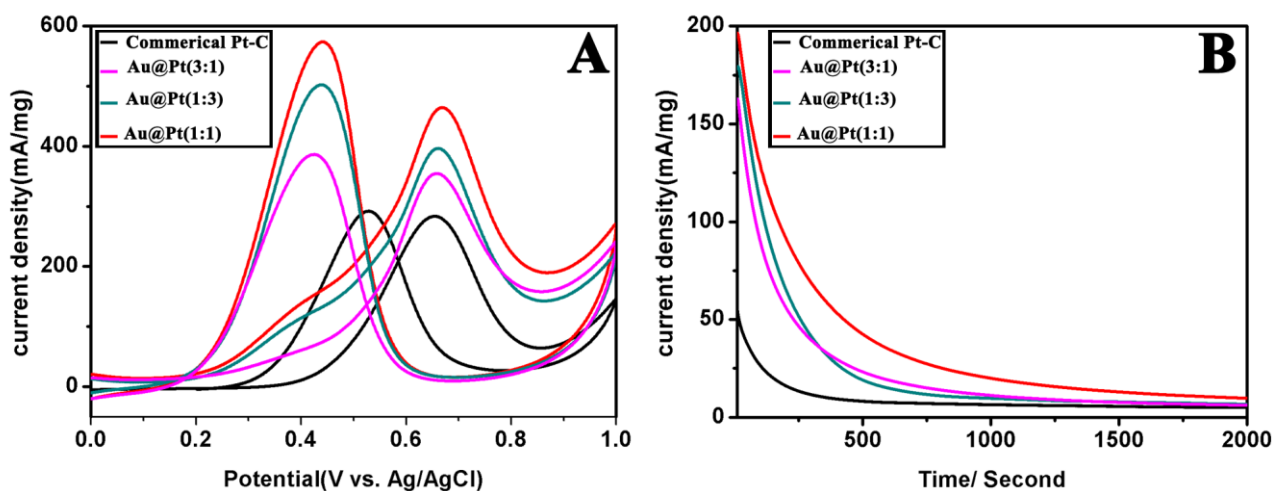


Figure 6. A The typical cyclic voltammograms (CVs) and B The time-current curve of NPs from different ratios of carbon-supported Au@Pt, carbon-supported Pt@Pt and carbon-supported commercial Pt; B Cyclic voltammograms at a scan rate of 20 mV/s. All measurements were carried out in a mixture of 0.5 M methanol and 0.5 M H₂SO₄ at 25°C.

4. SUMMARY

In conclusion, we demonstrate that carbon-supported Au@Pt nanocatalysts can be prepared via a surfactant-free seeded growth. Besides, the shell thickness of Pt can be tuned through controlling the amount of Pt precursor. This method is low-cost, simple and straightforward for large scale production. More importantly, these prepared catalysts show higher catalytic activity and stability in the electrocatalytic Oxidation of methanol than commercial carbon-supported Pt catalyst. Therefore, this method might have application in fuel cell.

Supporting Information:

Hydrogen absorption/dehydrogenation peak of the CV curve of the catalyst at different temperatures of CV curves will also appear in the supporting information. Form **Figure 7**. The higher catalytic activity of the catalyst at 60°C.

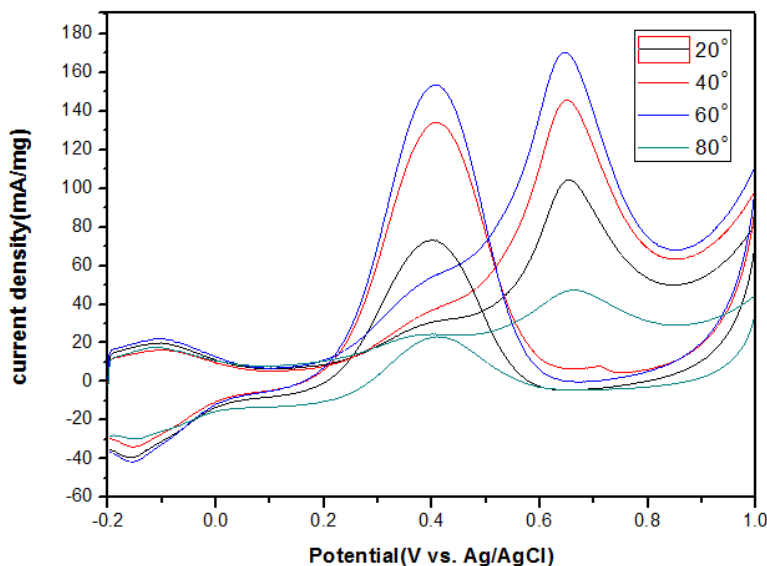


Figure 7. Hydrogen absorption/dehydrogenation peak of the CV curve of the NPs (carbon-supported Au@Pt) at different temperatures. Cyclic voltammograms at a scan rate of 20 mV/s. All measurements were carried out in a water.

ACKNOWLEDGEMENT

This work was supported by the from NSFC for outstanding young scientist (51025207), NSFC (21101120), Zhejiang science and technology project (2010C31039), Lucheng science and technology project (T100106), the National Natural Science Foundation of China (Grant No. 51263006/E031301), the Hainan Province Natural Science Foundation of China (Grant No. 211009).

Reference

1. (a) S. U.Son, Y. Jang, J. Park, H. B.Na, H. M.Park, H.J.Yun, J.Lee, and T.Hyeon, *J. Am. Chem. Soc.*, 126(2004)5026. (b) C. H.Jun, Y. J.ParK, Y. R.Yeon, J. R.Choi, W. R.Lee, S. J.Ko, and J. Cheon, *Chem. Commun.* (2006) 1619. (c) K.Meada, K.Teramura, D. L.Lu, N.Saito, Y.Inoue, and K. Domen, *Angew. Chem., Int. Ed.*,45(2006)7806.
2. J. W.Hu, J. F.Li, B.Ren, D.Y.Wu, S.G.Sun, and Z.Q.Tian, *J.Phys.Chem.C*, 111(2007)1105.
3. a: V.R.Stamenkovic, B.Flowler, B.S.Mun, G.F.Wang, P.N.Ross, C.A.Lucas, and N.M.Markovic, *Science* 315(2007)493. b. V.R.Stamenkovic, B.S.Mun, K.J.J.Mayrhofer, P.N.Ross, and N.M.Markovic, *J.Am.Chem.Soc.* 128(2006)8813.
4. T. Hyeon, *Chem. Commun.*, 2003(8) 927.
5. L. Yang, J. Chen, X. Zhong, K. Cui, Y. Xu, and Y. Kuang, *Colloids and Surfaces A: Physicochemical and Engineering Aspects.*, 295(2007) 21.
6. J.M. Yan, X.B. Zhang, T. Akita, M. Haruta, and Q. Xu, *J. Am. Chem. Soc.*, 132(2010)5326.
7. H.L. Jiang, T. Akita, T. Ishida, M. Haruta, and Q. Xu, *J. Am. Chem. Soc.* 133 (5)(2011) 1304.

8. N.Toshima, H.Yan, .Y.Shiraishi, B. Corain, G. Schmid, N.Toshima, N. Eds ,and B.ElsevierV, *Amsterdam*, 49 (2004)75.
9. X.W. Li, J.Y. Liu, W. He, Q.H. Huang, and H. Yang, *J. Colloid Interface Sci.* ,344 (2010)132.
10. J.H. Zeng, J. Yang, J.Y. Lee, and W.J. Zhou, *J. Phys. Chem. B*, 110 (2006) 24606.
11. H.A. Esfahani, L. Wang, and Y. Yamauchi, *Chem. Commun.*, 46 (2010) 3684.
12. H.Lang ,S. Maldonado ,K, Stevenson , and B. Chandler ,*J .Am .Chem .Soc.*, 126(2004)12949.
13. A.Villa ,C. Campione ,and L.Prati , . *Prati-Catal Lett.*, 06 (2007)133.
14. D.Mott, J.Luo, P. N.Njoki, Y.Lin, L.Wang, and C.J.Zhong, *Catal. Today.*, 122(2007) 378.
15. J.Luo,L.Wang,D.Mott,P.N.Njoki,Y.Lin,T.He,Z.Xu,B.N.Wanjala,and I.S.Lim,C.J.Zhong,*Adv.Mater.*, 20(2008)4342.
16. D. Mott, J.Luo, A.Smith, P.Njoki, L.Wang,and C. J.Zhong, *Nanoscale Res. Lett.* ,2(2007)12.
17. K.Zhang, Y.Xiang, X.Wu, L.Feng,W.He, J.Liu, W.Zhou, and S.Xie, *Langmuir*, 25(2009) 1162.
18. F.Bao, J. F.Li, B.Ren,J. L. Yao, R. A.Gu, and Z. Q.Tian, *J. Phys. Chem. C*, 112(2008)345.
19. Y.Chen,F.Yang, Y.Dai, W. Wang, and S.Chen,*J.Phys.Chem.C*, 112(2008)1645.
20. S. I.Sanchez, M. W.Small, J. M.Zuo, and R. G.Nuzzo, *J. Am. Chem. Soc.*, 131(2009)8683.
21. S. H.Johnson, C. L.Johnson, S. J.May, S.Hirsch, M. W.Coleb, and J. E. Spanier, *J. Mater. Chem.*, 20(2009)439.
22. Z. M. Peng, J. B. Wu, and H. Yang,*Chem. Mater.* , 22(2010)1098.
23. D.Zhao, and B.Q.Xu, *Angew. Chem. Int. Ed.*, 45(2006) 4955.
24. K. J.Carroll, S.Calvin, T. F.Ekiert, K. M.Unruh, and E. E.Carpenter, *Chem. Mater.*, 22(2010)2175.
25. Z.Fang, Y.Zhang, F. Du, and X.Zhong, *Nano Res.*, 1(2008) 249.
26. L.Cao, L.Tong, P.Diao, T.Zhu, and Z. Liu, *Chem. Mater.*,16(2004)3219.
27. Z.Peng, and H. Yang, *J. Am. Chem. Soc.*, 131(2009)7542.
28. (a) F.Fan,D. Liu, Y.Wu, S.Duan,Z.Xie, Z.Jiang, and Z.Tian, *J. Am. Chem. Soc.*, 130(2008)6949. (b) B.Lim, J.Wang, P. H. Camargo,C.M.Jiang, M.Kim, and Xia, Y.*Nano Lett.* ,8(2008) 2535.(c) D.Ferrer, A.T.Castro, X.Gao, S.S. Guzm,U.O.Mendez, and J.M.Yacam *Nano Lett.* 7(2007)1701
29. Y.Mu, H.Liang, J.Hu, L.Jiang, and L.Wan, *J. Phys. Chem. B.*, 109(2009)22212.
30. (a) E.Reddington, A.Sapienza, B.Gurau, R.Viswanathan, S.Sarangapani, E. S.Smotkin, and T. E. Mallouk, *Science* 280(1998)1735.(b) T.Hyeon, S.J.Han, Y. E. Sung, K. W.Park, and Y. WKim, *Angew.Chem., Int. Ed.* ,42(2003)4352.
31. J. Watt, S. Cheong, M. Toney, B. Ingham, J. Cookson, P. T. Bishop,and R. D. Tilley,*ACS Nano.* 4(2010)396.
32. M. Mahmoud, C. Tabor, M. El-Sayed, Y. Ding, and Z. Wang, *J. Am. Chem. Soc.* , 130(2008) 4590
33. J.Zeng, J.Yang, J.Lee, and W. Zhou, *J. Phys. Chem. B.*, 110(2006)24606.